Original Article
Food Science and Technology

ISSN 0101-2061 (Print)
ISSN 1678-457X (Online)

DOI: https://doi.org/10.1590/fst.65621

Ivermectin induces mitophagy in H9c2 cells via activation of the PINK1/Parkin pathway

Yanmin JIA[1]*, Baoxue HAN[2], Rene WANG[3]

Abstract

Ivermectin (IVM), a remarkable broad-spectrum anthelmintic and insecticides, which also contributes to clinical application. However, IVM induction of cytotoxicity through mitophagy has not been consistently proven in vitro. Here we investigate the cytotoxic effects of ivermectin in mammalian nontarget cells. We have used cck-8 assay to evaluate the cell viability. The Fluorescence labeling was detected the occurrence of autophagy and mitophagy. The ATP bioluminescence detection kit was used to detect changes in intracellular ATP levels. In addition, the western blot assay was applied to reflect the expression of autophagy-related and mitophagy- related proteins. Cellular calcium concentration analysis was captured with a flow cytometer. We also used western blot to reveal expression of the lysosomal membrane protein Lamp2. The expression of lysosomal cathepsin mRNA was evaluated by RT-PCR. The cell viability was significantly diminished in H9c2 cells and the number of autophagosomes increases in a dose-dependent way, at the same time, LC3-II / I ratio was increased. We also found that the H9c2 cellular ATP level was decreased and observed the mPTP opening. The co-localization of mitochondria and lysosomes was detected, also, we found the concentration of Ca^{2+}, the expression of Lamp 2 and mRNA expression levels of Cathepsin B and Cathepsin L significantly increased in a dose-dependent way in H9c2 cells. Finally, the results of expression of PINK1 and Parkin protein increased simultaneously in H9c2 cells. IVM induced mitophagy in H9c2 cells via PINK1/Parkin signaling.

Keywords: ivermectin; cytotoxicity; mitophagy; PINK1/Parkin.

Practical Application: Here, our study was revealed the underlying mechanism of IVM in H9c2 cells, which will construct a theoretical basis for us to find out the underlying molecular mechanism. We assesed whether IVM are able to regulate mitophagy through PINK1/Parkin signaling pathway. The results showed that IVM has potential cytotoxicity, which will have a risk of endanger mammalian health. Our work build a basis of potential molecular mechanism of IVM in non-targeted cells, which could provide more accurate view of IVM in other researches.

1 Introduction

Ivermectin (IVM), a mixture of more than 80% 22,23-dihydroavermectin B1a and approximately 20% 22,23-dihydroavermectin B1b, was well-known anti-helminthic agent from the late-1970s (Yang et al., 2020). William C. Campbell and Satoshi Ömura was awarded by Nobel Prize in Physiology and Medicine because of their discoveries leading to ivermectin in 2015 (Ōmura, 2016). The IVM have extraordinary efficacy against parasitic diseases such as river blindness, elephantiasis and scabies (Ashour, 2019; Vos et al., 2012). In addition, IVM has the ability to re-treat new diseases and will continue to offer new clinical applications (Formiga et al., 2021). The report confirmed that IVM has great antiviral activity against West Nile virus (also flavivirus) even in the low dosage. Before the US Food and Drug Administration (FDA) recently approved moxidectin for the treatment of human onchocerciasis in June 2018, IVM was the only member of ML approved for use in humans. The mechanism of IVM was caused accumulation of gamma amino butyric acid (GABA)-gated-Cl– channels, contributing a long-lasting hyperpolarization and paralysis of the infesting organism (Santos et al., 2009).

Although the use of IVM was significantly increased, there was no serious incident have been reported because of the use of IVM. However, there were reported that IVM may contribute to human headache, dizziness, muscle pain, nausea or diarrhea (Bai & Ogbourne, 2016). Also, the residue of IVM in meat, milk and other aninmal product was posed a risk potential to human healthy when used as pesticide (Escribano et al., 2012). In 2009, the European Union set a deadline for terminating IVM from edible organizations 49 days ago. Therefore, this purpose of this paper was to trace the mechanisms of mitophagy induced by IVM and characterize the disadvantages of IVM for human health.

Autophagy, a strictly regulated lysosomal-dependent protein degradation pathway that participates in the renewal of intracellular material and maintains cell homeostasis. Autophagy, a biological program in which cells degrade their internal senescent or damaged organelles, invading pathogens and misfolded proteins (Cheng et al., 2013). It is an indispensable part of the cell growth and development of multicellular organisms, structural reconstruction, and maintenance of cell homeostasis. Atg8/LC3 is

Received 01 Aug., 2021
Accepted 21 Aug., 2021
[1]*Department of Health Professional 1 Ward, Jinan Central Hospital, Jinan City, Shandong P.R., 250100, China*
[2]*Department of Hematology and Rheumatology, Jinan Central Hospital, Jinan City, Shandong P.R., 250100, China*
[3]*Department of Nursing, Jinan First People's Hospital, Jinan City, Shandong P.R., 250011, China*
*Corresponding author: drjiayanmin@163.com

an ubiquitin-like protein, which is converted from LC3-I to LC3-II by post-translational modification (Gai et al., 2013). LC3-II is distributed in autophagy vesicles and autophagosomes, and is a biomarker of autophagy. The bilayer membrane of autophagic vesicles continues to extend and closes under the mediation of Atg8/LC3-II to form autophagosomes (Kuma et al., 2007).

Mitochondria are the major energy resource required for cell vital activity and play an important role of cell regulating metabolism. Mitophagy, a selective autophagy, which participates in damaged or excess mitochondria removal (Eiyama et al., 2013). When mitochondria under adverse conditions such as oxidative stress, nutrient deficiency, and reduction of growth factors, the mitochondrial permeability transition pore (mPTP) was opened and increased mitochondrial permeability, accompanied by depolarization of the mitochondrial outer membrane. membrane permeabilization, MOMP) (Cao et al., 2011). There is evidence that changes in mitochondrial permeability may be involved in the selective autophagy of mitochondria (Youle & Narendra, 2011). PTEN-induced virtual kinase 1 is a serine / threonine protein kinase which can recognize damaged mitochondria and accumulate in the depolarized outer mitochondrial membrane. Under normal circumstances, PINK1 is introduced into the mitochondria in a mitochondrial membrane potential-dependent manner, and its N-terminal transmembrane region is inserted into the inner mitochondrial membrane. In addition, it is cleaved by the protease PARL (presenilin-related rhombus) on the inner mitochondrial membrane, and the C-terminal fragment returns The cytoplasm is degraded by proteases. PINK1 can also be degraded in the mitochondrial matrix. When the mitochondria are depolarized, the introduction of PINK1 into the mitochondria is blocked and the accumulation of the outer mitochondrial membrane is followed by the recruitment of Parkin from cytoplasm to the outer mitochondrial membrane and phosphorylation. Parkin has ubiquitin E3 ligase activity and ubiquitinates a variety of mitochondrial outer membrane proteins (Bingol & Sheng, 2016).

In this work, we used as model the rat cardiomyocyte H9c2 cell line, it was used widely to evaluate cytotoxicity in vitro. In our context, we assesed whether IVM are able to regulate mitophagy through PINK1/Parkin signaling pathway. The results showed that IVM has potential cytotoxicity, which will have a risk of endanger mammalian health.

2 Materials and methods

2.1 Chemicals

Ivermectin (CAS: 70288-86-7, Sigma-Aldrich (St. Louis., MO, USA,Inc:PHR1380), monodansylcadaverine (MDC), RIPA lysis buffer, N,N,N'N'-tetramethylethylenediamine (TEMED), 2-amino-2-(hydroxymethyl)-1,3-propanediol (Tris), and phenylmethylsulfonyl fluoride (PMSF) were purchased from Bio-Rad Laboratories, Inc.(NYSE:BIO); LC3, PINKI, Parkin, Lamp2 and β-actin antibodies were obtained from Sigma-Aldrich (St. Louis, MO, USA); Cell Counting Kit-8, ATP kit, Mito-Tracker Green, and Lyso-Tracker Red were obtained from Beyotime Institute of Biotechnology (Shanghai, China); TRNzol reagent and Secondary anti-rabbit antibody was bought from Sangon Biotech Co., Ltd (Shanghai, China); Reverse Transcription Kit and SYBR green qPCR Master Mix were obtained from Takara (Dalian, China); Other chemicals used were of analytical grade and purchased locally.

2.2 Cell culture

The H9c2 cell line was purchased from American Type Culture Collection (ATCC, CRL-1446, USA). We cultured cells at a 25 cm^2 flask supplemented and incubated at 37 °C with 5% (v/v) CO_2.The cell medium was used with Dulbecco's Modified Eagle's Medium, and 10% heat-inactivated FBS, 100 units/mL penicillin sodium, 100 mg/mL streptomycin solution (Gibco, Grand Island, NY, USA). Exponentially growing cells were used in all researches.

2.3 Cell viability assay

H9c2 suspensions were pipetted 100 μL to 96-well plate. After 6 h of incubation, IVM were added for each well at 0, 1, 2, 4, 8 μmol/L. Four hours prior to the assay, 10 μL of CCK-8 solution was added to each well. The solution was gently mixed in an orbital shaker for 1 minute to ensure a uniform distribution of colors. Then measure the optical density using a microplate reader (BioTek, Winooski, VT, USA) with a wavelength at 450 nm.

2.4 Fluorescence microscopy

H9c2 cell suspensions (1×10^6 cells/well) were seeded in 6 well culture plate (Nest Biotech, China) and incubated overnight and were treated with IVM at 0, 1, 2, 4, 8 μmol/L. Cells were washed with PBS and then loaded with MDC, Mito-Tracker Green, and Lyso-Tracker Red to respectively detect the autophagosomes, mitochondria, and lysosomes of cells. The fluorescence microscope was used to observe the cells. (Leica, Wetzlar and Mannheim, Germany).

2.5 Western blot assay

After treatment with 0, 1, 2, 4, 8 μmol/L IVM for 6 h, H9c2 cells were washed twice with cold PBS, dissociated with RIPA buffer on 4 °C, then the cells were centrifuged at 12,000g, 4 °C in centrifuging for half an hour. Cellular concentration of protein was reflectd by the BCA protein assay kit. Samples were equivalent segregate by 8% -12% SDS-polyacrylamide gel electrophoresis (SDS-PAGE) and then transferred to PVDF membranes. The membranes were blocked with 5% non-fat dry milk dissolved in TBST (10 mM Tris-HCl, 150 mM NaCl, 0.1% Tween-20, pH 7.5) for 2 h at room temperature. Then, the bands were incubated overnight with HRP-binding secondary antibody using the primary antibody (1: 1000) diluted on ice and were visualized with enhanced chemiluminescence (ECL) reagent (Tanon, Shanghai, China).

2.6 ATP determination

The ATP bioluminescence detection kit was used to detect changes in intracellular ATP levels according to the protocol (BioTek, Winooski, VT, USA). H9c2 cells were seeded in a Φ10cm cell culture plate with 1×10^7 cells per dish. Incubate for 24 hours in the incubator, pour out the culture medium in each culture well. The control group was added with 7 mL of fresh medium,

and the treatment group was added with an equal amount of medium containing spinosyn at a concentration of 0, 1, 2, 4, 8 μmol/L respectively and 6 hours After incubation, the cells of each group were harvested by centrifugation, 500 μL of ATP detection lysate was added to the cell pellets of each group, and after full lysis, centrifuged at 12000 × g, 4 °C for 20 minutes to take the supernatant. The ATP detection reagent 1:9 with the ATP detection reagent diluent to obtain ATP detection working solution. 100 μL of ATP working solution was added to a black 96-well plate at room temperature for 4 minutes. Add 10 μL of protein sample solution to each well, mix quickly, and place in a microplate reader to detect the intensity of self-luminescence.

2.7 Mitochondrial permeability transition pore(mPTP) assay

IVM was added to the cells at the concentrations of 0, 1, 2, 4, 8 μmol/L. Then, the cells were loaded with 1 mmol/L calcein-AM at 37 °C for 0.5h and then add 1mmol/L $CoCl_2$ at 37 °C for 0.5h. After washed with PBS) twice, the fluorescence images were obtained through fluorescence microscope. (Leica, DM3000, Wetzlar and Mannheim, Germany).

2.8 Flow cytometry

Cellular calcium concentration analysis was captured with a flow cytometer (FACS Calibur, Becton Dickinson) recording to the method of Sawai and Domae. After incubated with IVM for 6 h at 0,1,2,4,8 μmol/L, the cells were centrifuging and washing with cold PBS twice then resuspended in 500 mL binding buffer (10 μmol/L HEPES, 140 μmol/L NaCl, 2.5 μmol/L CaCl2, pH 7.4). The cell suspension was incubated with 5 mL Fluo 3-AM at 37 °C for 30 min, after staining, cells were re-suspended in binding buffer and ascended using the flow cytometer with the accompanying Cell Quest software procedure.

2.9 Q-PCR analysis

After being treated with IVM for 6 h at 0, 1, 2, 4, 8 μmol/L, the TRNzol reagent was used to extract the RNA of cells according to protocol. The RNA concentration was analyzed by microplate reader (BioTek, Winooski, VT, USA). The Reverse Transcription Kit was used to reverse transcribed to cDNA. The templates of cDNA were detected with a SYBR Green PCR Kit by real-time PCR (BIO-RAD, USA). The expression gene data were normalized by b-actin expression.

2.10 Statistical analysis

The data are represented as mean ± standard deviation. One-way analysis was used to statistically significance of the difference of each sample. The significance of the difference between the groups was determined by T-test. p value below 0.05 is considered as statistically significant.

3 Results

3.1 The effect of H9c2 cytotoxicity induced by IVM

The cell viability of H9c2 cells treated with IVM for 6 h was assessed by CCK-8 assay. The results showed that after being treated with IVM, the cell viability was significantly diminished when compared with the control group (Figure 1). The IC50 value of IVM treatments at 6 h was approximately 1.98 μmol/L as determined from the cell growth curve,. The result showed that the IVM could inhibited the cell viability.

3.2 IVM induced autophagy in H9c2 cells

MDC is an eosinophilic fluorescent stain that can stain acidic vacuoles in cells and presented distributed spots in the cytoplasm. The MDC is often used as a preliminary detection of autophagic lysosome formation. After treated with IVM for 6 h, the number of autophagosomes increases in a dose-dependent way as shown in Figure 2A. These data suggested IVM formed autophagosomes in H9c2 cells.

In addition, LC3 is considered as a marker protein of autophagosome membranes owing to its' ability of binding to lipid molecules of autophagosomes and autophagosome membranes. In normal cells, LC3 existed in the form of LC3-II, which is dispersed throughout the cytoplasm. Once autophagy occurred, LC3-II is converted into LC3-I through lipidation and is recruited to the autophagosome membrane to promote the extension and maturation of the autophagosome. As shown in Figure 2B, the results confirmed that the LC3-II/I ratio increases in a dose-dependent way, and IVM induce autophagy by upregulating LC3-II expression levels. These results illustrate that IVM induced autophagy in H9c2 cells.

3.3 IVM induced mitochondrial damage in H9c2 cells

In the presence of ATP, firefly luciferase catalyzes the emission of photons from the luciferin substrate. Within a certain concentration range, the fluorescence intensity emitted is proportional to the concentration of ATP. The ATP bioluminescence detection kit was used to detect the changes in the ATP level in the cell lysis protein solution. As expected, the ATP level in H9c2 cells affected by IVM was significantly decreased. After being treated with 0, 1, 2, 4, 8 μmol/L IVM for 6 hours, the content of cellular ATP decreased by 87.90%, 53.39%, 25.74%, 12.16% compared with the control group % (Figure 3A).

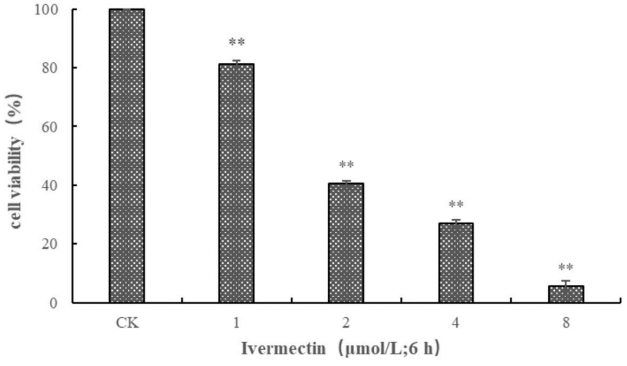

Figure 1. IVM inhibited the cell viability of H9c2 cells. each value is the mean ± SD. CK group: H9c2 cells cultured without IVM. *p < 0.05, **p < 0.01.

The Calcein-AM/CoCl2 fluorescence experiment was used to detect the openness of mPTP. First, IVM was used to added to H9c2 cells for, respectively. With the prolongation of action time, the fluorescence in the mitochondria was increased, indicating that the concentration of Ca^{2+} in the mitochondria continued to increase and reached 4 μmol/L after the treatment. The increase of the Ca^{2+} concentration in the mitochondria contributed to mPTP opening, Ca^{2+} outflows from the mitochondria and the inflow of cytoplasmic Co^{2+}, the fluorescence intensity of calcein in the mitochondria decreases (Figure 3B).These results demonstrated that IVM induced mitochondrial damage in H9c2 cells.

3.4 IVM induced mitophagy in H9c2 cells

The process of damaged and dysfunctional mitochondria is specific. Through the selective uptake of autophagosomes, mitochondria are finally transported to lysosomes for degradation. The results were shown in Figure 4. Mito-Tracker Green-labeled mitochondria and Lyso-Tracker Red-labeled lysosomes. We found that cells were separated, and the cells did not co-localize in the control group. After treated with 0, 1, 2, 4, 8 μmol/L IVM for 6 h, the green fluorescence of the labeled mitochondria and the red fluorescence of the labeled lysosome were superimposed,

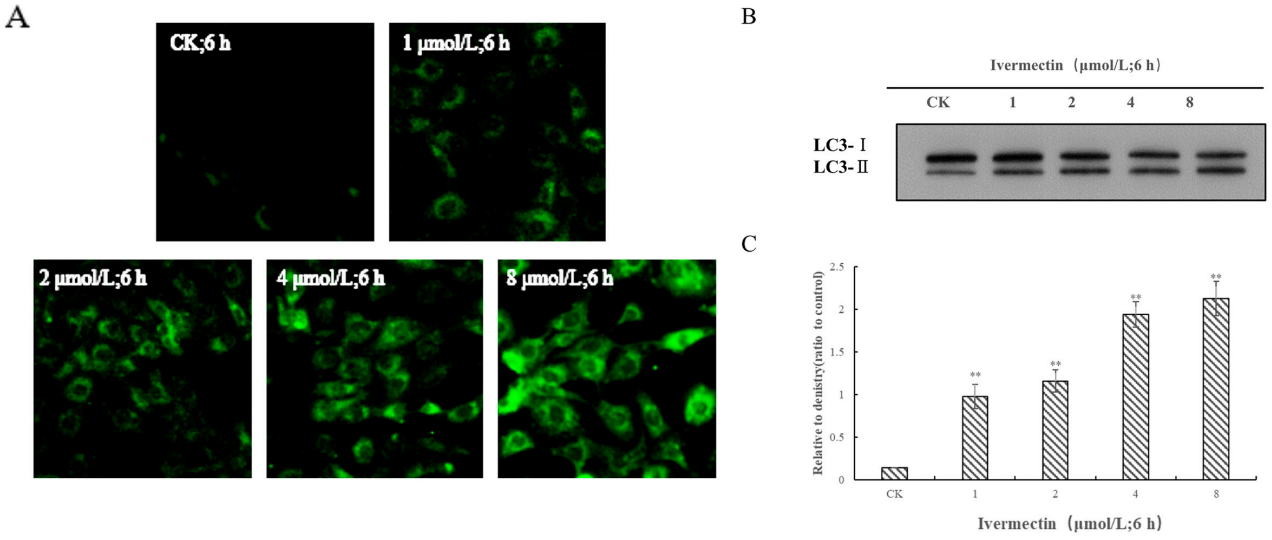

Figure 2. IVM induced autophagy in H9c2 cells. (A) H9c2 cells were treated with IVM for 6 h and then incubated with MDC, the autophagosome were analyzed by fluorescence microscopy; (B) After treated with IVM for 6 h, the expression of autophagy-associated proteins LC3 in H9c2 cells were detected by western blot; (C) Densitometry evaluation of three independent experiments was carried out, each value is the mean ± SD. *p < 0.05, **p < 0.01. The data shown are the mean from three independent experiments. Each value is the mean ± SD of three determinations.

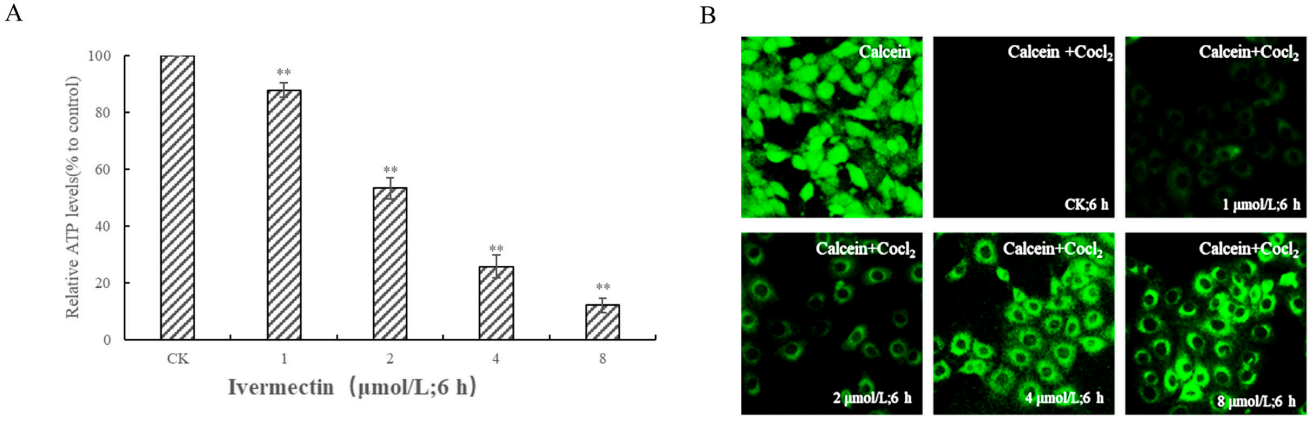

Figure 3. IVM induced mitochondrial damage in H9c2 cells. (A) After treated with IVM for 6 h, ATP content was measured. All the experiments were performed in triplicates, each value is the mean ± SD. *p < 0.05, **p < 0.01; (B) After treated with IVM for 6 h, the mPTP opening was detected by co-loading with calcein-AM and CoCl2.

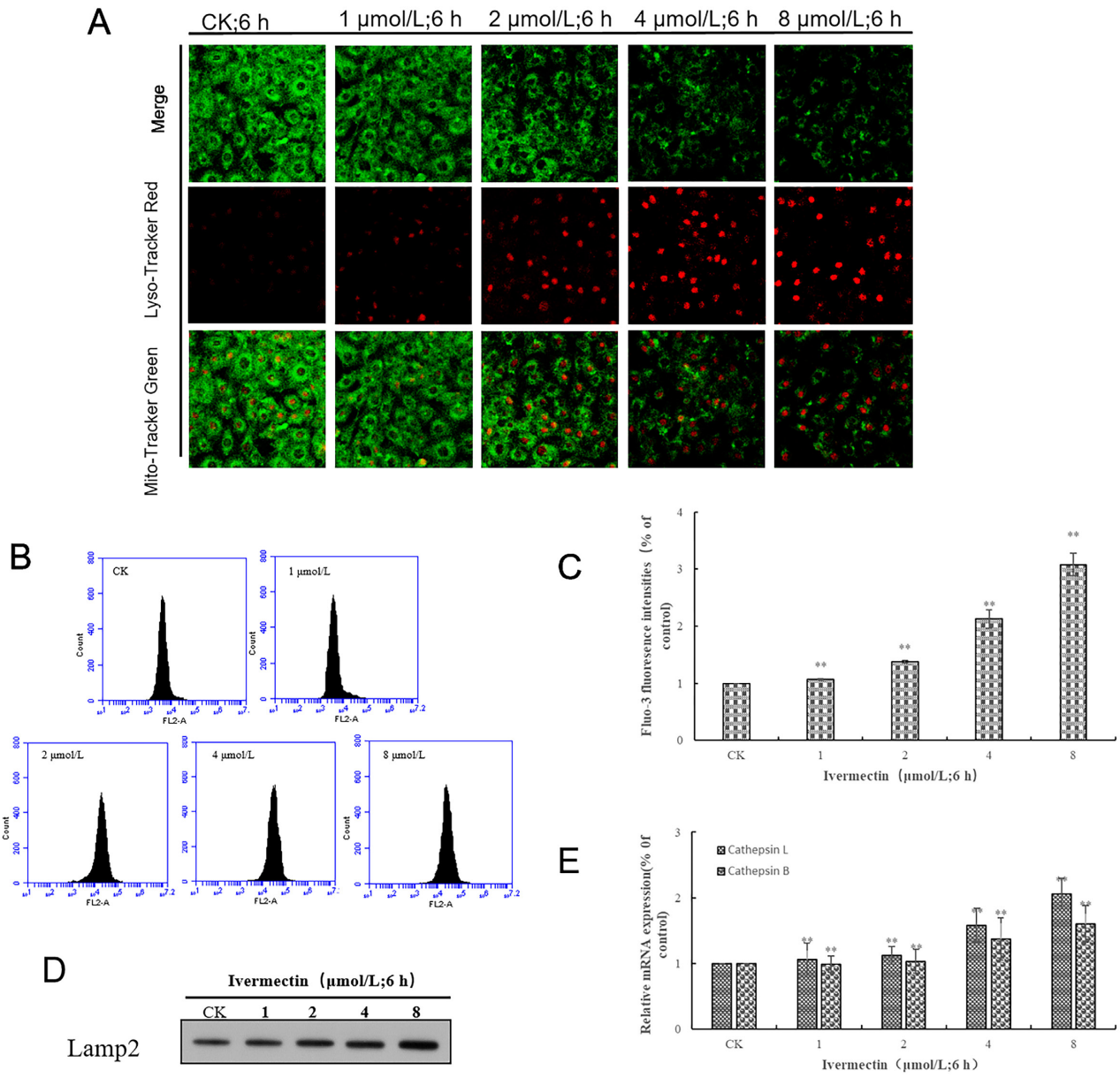

Figure 4. IVM induced mitophagy in H9c2 cells. (A) After treated with IVM for 6 h, mitochondria and lysosomes were stained with Mito-Tracker and Lyso Tracker Red, then detected by fluorescence microscopy; (B) The Ca2+ was labeled with Fluo 3-AM fluorescence probes and measured by microplate reader; (C) Fluo-3 fluorescence intensities; (D) After treated with IVM for 6 h, the expression of Lamp2 in H9c2 cells were detected by western blot; (E) The expression of Cathepsin B and Cathepsin L mRNA were evaluated by RT-PCR. Densitometry evaluation of three independent experiments was carried out. The data shown are the mean from three independent experiments. Each value is the mean ± SD of three determinations. *$p < 0.05$, **$p < 0.01$.

representing a yellow fluorescent spot. Which indicated that co-localized of autophagosomes and lysosomes, and the mitochondria would be degraded in the lysosome (Figure 4A).

When cells stimulated by intracellular and extracellular signals, which will leaded to an increase in the concentration of intracellular free Ca^{2+}, which in turn triggers a series of Ca^{2+}-dependent signal transduction. The result was shown in Figure 4B. After the H9c2 cells loaded with Fluo3-AM are subjected to IVM, the intracellular Ca^{2+} concentration instantly increases. This result confirmed that IVM-induced increase OF Ca^{2+} concentration in H9c2 cells.

Lamp 2 is a lysosomal transmembrane protein that exists in the process of autophagosome fusion with lysosome and the formation of autophagolysosome. H9c2 cells were treated with 0, 1, 2, 4, 8 μmol/L IVM for 6 h and the test result was shown in Figure 4C. The expression of Lamp 2 was increased and

shown in a dose-dependent way. Which indicated the clearance of damaged mitochondria induced by IVM is related to the formation of autophagolysosomes.

Cathepsin is an important proteolytic enzyme system in lysosomes, mainly involved in the degradation of intracellular organelles and proteins. Cathepsin B and Cathepsin L were involved in the regulation of programmed cell death.We evaluated the expression of Cathepsin B and Cathepsin L at the mRNA level by RT-PCR, the result is shown in Figure 4E. As shown in Figure 4D, when H9c2 cells exposed to IVM 0, 1, 2, 4, 8 μmol/L respectively, the mRNA expression levels of Cathepsin B and Cathepsin L significantly increased in a dose-dependent way. This result suggested that IVM induced the increase the activity of lysosomes in H9c2 cells, which is beneficial to the removal of damaged mitochondria. Moreover, this result ensured IVM-induced mitophagy in H9c2 cells at the molecular level.

3.5 Effects of IVM on PINK1/Parkin signaling pathways in H9c2 cells

PINK1 and Parkin proteins are important biological markers of mitophagy. In order to further confirm signaling pathways of IVM-induced mitophagy in H9c2 cells, Western blot was used to assess PINK1 and Parkin proteins expression. As shown in Figure 5, the expression of PINK1 and Parkin protein increased simultaneously in a dose-dependent way. This result revealed that IVM-induced PINK1/Parkin mitochondrial signal transduction pathway activated.

4 Discussion

Usually, most researchers believed that the advantages of IVM in global public health and socio-economic well-being are endless and still accumulating (Gupta et al., 2020; Tang et al., 2021). With the increased worldwide use of IVM, the report showed that IVM has overcome many parasitic diseases infecting millions of people, such as strongyloidiasis and onchocerciasis (Martin et al., 2021). However, IVM is categorized as highly toxic with acute oral and dermal toxicity of category I and II respectively (Imperiale et al., 2004). The report noted that chronic and subchronic toxicity under low IVM exposure may be of greater concern (Laing et al., 2017). However, there is little known about the degree of potential toxicity to humans or higher animals, as there are currently no reliable studies. Hence, we studied that whether IVM has potential toxicity in mammal cells.

To evaluate its biological safety on mammalian cells, we analysis the cell viability of IVM on H9c2 cells by CCK-8. The results revealed that IVM decreased the cell viability a dose-dependent way (Figure 1). This illustrated that IVM has cytotoxicity to cells in vitro, this might be the basis for potential risks to mammals. Therefore, a wide range of concentrations and 6 hours were used to reflect the mitochondrial inducing effect of IVM on H9c2 cells. Autophagy is considered as a mechanism of cell survival, however, studies have also indicated that autophagy is associated with cell death recently (Jung et al., 2008). Whether autophagy promotes cell survival or cell death depends on the intensity of the stimulation on cells. Our research found that IVM have induced autophagy in H9c2 cells, and

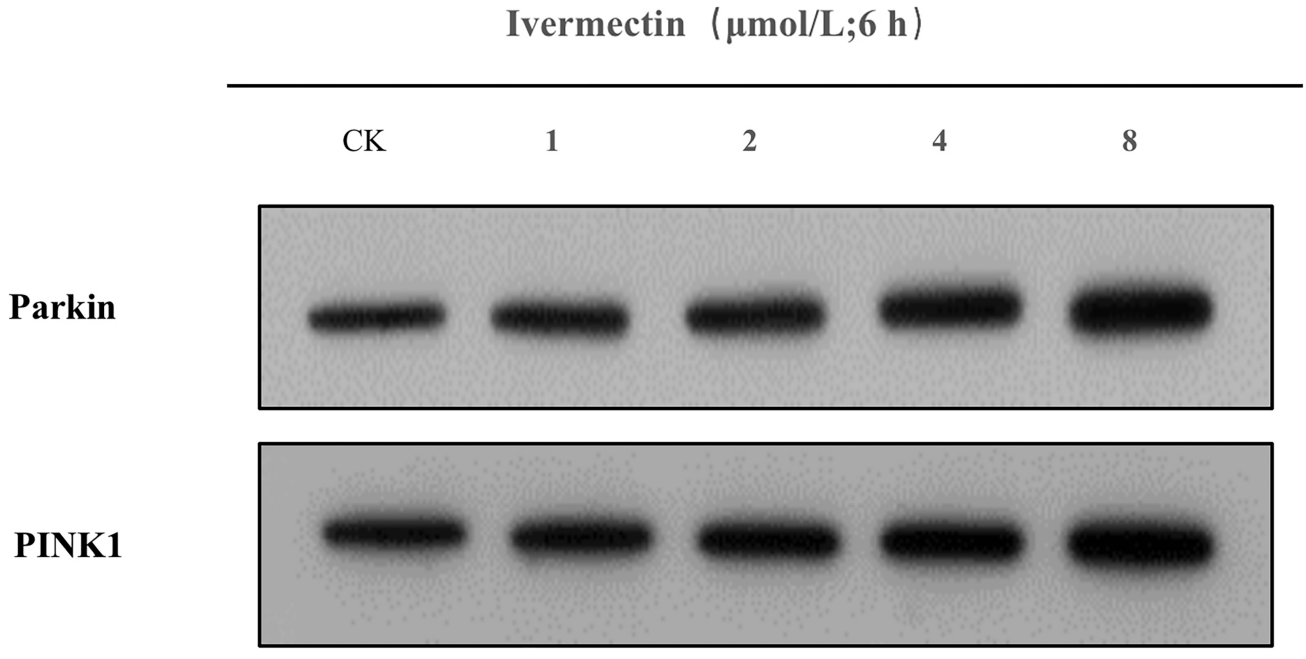

Figure 5. IVM induced the Parkin/PINK1 signaling pathways in H9c2cells. After treated with IVM for 6 h, representative western blot analyses of phosphorylation of Parkin, PINK1in H9c2 cells were performed.

the molecular mechanism has been preliminary explored. The results of MDC staining revealed that IVM significantly increased the autophagy level of H9C2 cells. Western blot was used to visualize the expression of autophagy-related proteins, the results further confirmed the autophagy-inducing effect of IVM on H9c2 cells (Figure 2).

Mitochondria is a necessary organelle for cells to carry out energy conversion and metabolic regulation and play a vital role in a variety of life activities such as Ca^{2+} homeostasis, cell death, cell cycle regulation and the body's natural immune response (Kim et al., 2007). Therefore, there is a strict mitochondrial quality control mechanism in cells to ensure the effective execution of metabolic functions and the timely start of programmed cell death. Mitophagy is the mitochondrial degradation pathway that depends on autophagy and is the core mechanism for mitochondrial quality control (Kobayashi & Liang, 2015). The results showed that the decrease in mitochondrial ATP content caused by IVM on H9c2 cells and the mPTP opened (Figure 3), which suggested that IVM induced mitochondrial damage. To further confirmed weather mitophagy was occurred, we detected the co-localization of mitochondria and lysosomes, which is a preliminary judgment of the occurrence of mitophagy (Zhang et al., 2010). Lamp protein is important protein to maintain the stability of lysosomal membrane structure and participates in the process of fusion of mature autophagosomes and lysosomes, Lamp 2 has more significant effect. Recent research results show that many autophagosomes can be observed in Lamp 2 protein-deficient cells, and the degradation of long-lived proteins is reduced, confirming that the increase of autophagosomes is caused by slowing down of degradation, rather than increased production (Yoshii & Mizushima, 2015). We also detected the increase of Lamp 2 protein expression and the increase of cathepsin gene expression, suggesting that lysosomes are involved in the clearance process of damaged mitochondria. In addition, we evaluated the expression changes of Cathepsin B and Cathepsin L by RT-PCR at the mRNA level which confirmed that IVM induced mitophagy at molecular level (Figure 5).

The ubiquitination of PINK1 and Parkin proteins has attracted much attention in the regulation of mitochondrial recognition. In this study, western blot assay wea used to notice the increase in expression of PINK1 and Parkin proteins. This result also confirmed the process of selective envelopment of damaged mitochondria by autophagic vesicles and demonstrated a possible mechanism of IVM-induced mitophagy via the PINK1/ Parkin pathway in H9c2 cells.

In conclusion, we are the first one to demonstrated that IVM induce mitophagy in H9c2 cells via PINK1/Parkin signaling. Our results also build a basis of potential molecular mechanism of IVM in non-targeted cells, which could provide more accurate view of IVM in other researches. However, it turns out that our research has its limitations. We should further study other factors of the mitophagy pathways to fully understand mechanisms of IVM.

Conflict of interes

The author(s) declared no potential conflicts of interest with respect to the research, authorship, and/or publication of this article.

Reference

Ashour, D. S. (2019). Ivermectin: From theory to clinical application. *International Journal of Antimicrobial Agents*, 54(2), 134-142. http://dx.doi.org/10.1016/j.ijantimicag.2019.05.003. PMid:31071469.

Bai, S. H., & Ogbourne, S. (2016). Eco-toxicological effects of the avermectin family with a focus on abamectin and ivermectin. *Chemosphere*, 154, 204-214. http://dx.doi.org/10.1016/j.chemosphere.2016.03.113. PMid:27058912.

Bingol, B., & Sheng, M. (2016). Mechanisms of mitophagy: PINK1, Parkin, USP30 and beyond. *Free Radical Biology & Medicine*, 100, 210-222. http://dx.doi.org/10.1016/j.freeradbiomed.2016.04.015. PMid:27094585.

Cao, X. H., Zhao, S. S., Liu, D. Y., Wang, Z., Niu, L. L., Hou, L. H., & Wang, C. L. (2011). ROS-Ca(2+) is associated with mitochondria permeability transition pore involved in surfactin-induced MCF-7 cells apoptosis. *Chemico-Biological Interactions*, 190(1), 16-27. http://dx.doi.org/10.1016/j.cbi.2011.01.010. PMid:21241685.

Cheng, Y., Ren, X., Hait, W. N., & Yang, J. M. (2013). Therapeutic targeting of autophagy in disease: biology and pharmacology. *Pharmacological Reviews*, 65(4), 1162-1197. http://dx.doi.org/10.1124/pr.112.007120. PMid:23943849.

Eiyama, A., Kondo-Okamoto, N., & Okamoto, K. (2013). Mitochondrial degradation during starvation is selective and temporally distinct from bulk autophagy in yeast. *FEBS Letters*, 587(12), 1787-1792. http://dx.doi.org/10.1016/j.febslet.2013.04.030. PMid:23660403.

Escribano, M., San Andrés, M. I., Lucas, J. J., & González-Canga, A. (2012). Ivermectin residue depletion in food producing species and its presence in animal foodstuffs with a view to human safety. *Current Pharmaceutical Biotechnology*, 13(6), 987-998. http://dx.doi.org/10.2174/138920112800399121. PMid:22039793.

Formiga, F. R., Leblanc, R., de Souza Rebouças, J., Farias, L. P., de Oliveira, R. N., & Pena, L. (2021). Ivermectin: an award-winning drug with expected antiviral activity against COVID-19. *Journal of Controlled Release*, 329, 758-761. http://dx.doi.org/10.1016/j.jconrel.2020.10.009. PMid:33038449.

Gai, Z., Zhang, X., Islam, M., Wang, X., Li, A., Yang, Y., Li, Y., Peng, J., Hong, H., & Liu, K. (2013). Characterization of Atg8 in lepidopteran insect cells. *Archives of Insect Biochemistry and Physiology*, 84(2), 57-77. http://dx.doi.org/10.1002/arch.21114. PMid:23959953.

Gupta, D., Sahoo, A. K., & Singh, A. (2020). Ivermectin: potential candidate for the treatment of COVID 19. *The Brazilian Journal of Infectious Diseases*, 24(4), 369-371. http://dx.doi.org/10.1016/j.bjid.2020.06.002. PMid:32615072.

Imperiale, F., Lifschitz, A., Sallovitz, J., Virkel, G., & Lanusse, C. (2004). Comparative depletion of ivermectin and moxidectin milk residues in dairy sheep after oral and subcutaneous administration. *The Journal of Dairy Research*, 71(4), 427-433. http://dx.doi.org/10.1017/S002202990400038X. PMid:15605709.

Jung, H. S., Chung, K. W., Won Kim, J., Kim, J., Komatsu, M., Tanaka, K., Nguyen, Y. H., Kang, T. M., Yoon, K. H., Kim, J. W., Jeong, Y. T., Han, M. S., Lee, M. K., Kim, K. W., Shin, J., & Lee, M. S. (2008). Loss of autophagy diminishes pancreatic beta cell mass and function with resultant hyperglycemia. *Cell Metabolism*, 8(4), 318-324. http://dx.doi.org/10.1016/j.cmet.2008.08.013. PMid:18840362.

Kim, I., Rodriguez-Enriquez, S., & Lemasters, J. J. (2007). Selective degradation of mitochondria by mitophagy. *Archives of Biochemistry and Biophysics*, 462(2), 245-253. http://dx.doi.org/10.1016/j.abb.2007.03.034. PMid:17475204.

Kobayashi, S., & Liang, Q. (2015). Autophagy and mitophagy in diabetic cardiomyopathy. *Biochimica et Biophysica Acta*, 1852(2), 252-261. http://dx.doi.org/10.1016/j.bbadis.2014.05.020. PMid:24882754.

Kuma, A., Matsui, M., & Mizushima, N. (2007). LC3, an autophagosome marker, can be incorporated into protein aggregates independent of autophagy: caution in the interpretation of LC3 localization. *Autophagy*, 3(4), 323-328. http://dx.doi.org/10.4161/auto.4012. PMid:17387262.

Laing, R., Gillan, V., & Devaney, E. (2017). Ivermectin: old drug, new tricks? *Trends in Parasitology*, 33(6), 463-472. http://dx.doi.org/10.1016/j.pt.2017.02.004. PMid:28285851.

Martin, R. J., Robertson, A. P., & Choudhary, S. (2021). Ivermectin: An Anthelmintic, an Insecticide, and Much More. *Trends in Parasitology*, 37(1), 48-64. http://dx.doi.org/10.1016/j.pt.2020.10.005. PMid:33189582.

Ōmura, S. (2016). A splendid gift from the earth: the origins and impact of the avermectins (Nobel lecture). *Angewandte Chemie International Edition in English*, 55(35), 10190-10209. http://dx.doi.org/10.1002/anie.201602164. PMid:27435664.

Santos, A. R., Falcão, C. A. B., Muzitano, M. F., Kaiser, C. R., Rossi-Bergmann, B., & Férézou, J.-P. (2009). Ivermectin-derived leishmanicidal compounds. *Bioorganic & Medicinal Chemistry*, 17(2), 496-502. http://dx.doi.org/10.1016/j.bmc.2008.12.003. PMid:19114308.

Tang, M., Hu, X., Wang, Y., Yao, X., Zhang, W., Yu, C., Cheng, F., Li, J., & Fang, Q. (2021). Ivermectin, a potential anticancer drug derived from an antiparasitic drug. *Pharmacological Research*, 163, 105207. http://dx.doi.org/10.1016/j.phrs.2020.105207. PMid:32971268.

Vos, T., Flaxman, A. D., Naghavi, M., Lozano, R., Michaud, C., Ezzati, M., Shibuya, K., Salomon, J. A., Abdalla, S., Aboyans, V., Abraham, J., Ackerman, I., Aggarwal, R., Ahn, S. Y., Ali, M. K., Alvarado, M., Anderson, H. R., Anderson, L. M., Andrews, K. G., Atkinson, C., Baddour, L. M., Bahalim, A. N., Barker-Collo, S., Barrero, L. H., Bartels, D. H., Basáñez, M. G., Baxter, A., Bell, M. L., Benjamin, E. J., Bennett, D., Bernabé, E., Bhalla, K., Bhandari, B., Bikbov, B., Bin Abdulhak, A., Birbeck, G., Black, J. A., Blencowe, H., Blore, J. D., Blyth, F., Bolliger, I., Bonaventure, A., Boufous, S., Bourne, R., Boussinesq, M., Braithwaite, T., Brayne, C., Bridgett, L., Brooker, S., Brooks, P., Brugha, T. S., Bryan-Hancock, C., Bucello, C., Buchbinder, R., Buckle, G., Budke, C. M., Burch, M., Burney, P., Burstein, R., Calabria, B., Campbell, B., Canter, C. E., Carabin, H., Carapetis, J., Carmona, L., Cella, C., Charlson, F., Chen, H., Cheng, A. T., Chou, D., Chugh, S. S., Coffeng, L. E., Colan, S. D., Colquhoun, S., Colson, K. E., Condon, J., Connor, M. D., Cooper, L. T., Corriere, M., Cortinovis, M., de Vaccaro, K. C., Couser, W., Cowie, B. C., Criqui, M. H., Cross, M., Dabhadkar, K. C., Dahiya, M., Dahodwala, N., Damsere-Derry, J., Danaei, G., Davis, A., De Leo, D., Degenhardt, L., Dellavalle, R., Delossantos, A., Denenberg, J., Derrett, S., Des Jarlais, D. C., Dharmaratne, S. D., Dherani, M., Diaz-Torne, C., Dolk, H., Dorsey, E. R., Driscoll, T., Duber, H., Ebel, B., Edmond, K., Elbaz, A., Ali, S. E., Erskine, H., Erwin, P. J., Espindola, P., Ewoigbokhan, S. E., Farzadfar, F., Feigin, V., Felson, D. T., Ferrari, A., Ferri, C. P., Fèvre, E. M., Finucane, M. M., Flaxman, S., Flood, L., Foreman, K., Forouzanfar, M. H., Fowkes, F. G., Franklin, R., Fransen, M., Freeman, M. K., Gabbe, B. J., Gabriel, S. E., Gakidou, E., Ganatra, H. A., Garcia, B., Gaspari, F., Gillum, R. F., Gmel, G., Gosselin, R., Grainger, R., Groeger, J., Guillemin, F., Gunnell, D., Gupta, R., Haagsma, J., Hagan, H., Halasa, Y. A., Hall, W., Haring, D., Haro, J. M., Harrison, J. E., Havmoeller, R., Hay, R. J., Higashi, H., Hill, C., Hoen, B., Hoffman, H., Hotez, P. J., Hoy, D., Huang, J. J., Ibeanusi, S. E., Jacobsen, K. H., James, S. L., Jarvis, D., Jasrasaria, R., Jayaraman, S., Johns, N., Jonas, J. B., Karthikeyan, G., Kassebaum, N., Kawakami, N., Keren, A., Khoo, J. P., King, C. H., Knowlton, L. M., Kobusingye, O., Koranteng, A., Krishnamurthi, R., Lalloo, R., Laslett, L. L., Lathlean, T., Leasher, J. L., Lee, Y. Y., Leigh, J., Lim, S. S., Limb, E., Lin, J. K., Lipnick, M., Lipshultz, S. E., Liu, W., Loane, M., Ohno, S. L., Lyons, R., Ma, J., Mabweijano, J., MacIntyre, M. F., Malekzadeh, R., Mallinger, L., Manivannan, S., Marcenes, W., March, L., Margolis, D. J., Marks, G. B., Marks, R., Matsumori, A., Matzopoulos, R., Mayosi, B. M., McAnulty, J. H., McDermott, M. M., McGill, N., McGrath, J., Medina-Mora, M. E., Meltzer, M., Mensah, G. A., Merriman, T. R., Meyer, A. C., Miglioli, V., Miller, M., Miller, T. R., Mitchell, P. B., Mocumbi, A. O., Moffitt, T. E., Mokdad, A. A., Monasta, L., Montico, M., Moradi-Lakeh, M., Moran, A., Morawska, L., Mori, R., Murdoch, M. E., Mwaniki, M. K., Naidoo, K., Nair, M. N., Naldi, L., Narayan, K. M., Nelson, P. K., Nelson, R. G., Nevitt, M. C., Newton, C. R., Nolte, S., Norman, P., Norman, R., O'Donnell, M., O'Hanlon, S., Olives, C., Omer, S. B., Ortblad, K., Osborne, R., Ozgediz, D., Page, A., Pahari, B., Pandian, J. D., Rivero, A. P., Patten, S. B., Pearce, N., Padilla, R. P., Perez-Ruiz, F., Perico, N., Pesudovs, K., Phillips, D., Phillips, M. R., Pierce, K., Pion, S., Polanczyk, G. V., Polinder, S., Pope, C. A. 3rd, Popova, S., Porrini, E., Pourmalek, F., Prince, M., Pullan, R. L., Ramaiah, K. D., Ranganathan, D., Razavi, H., Regan, M., Rehm, J. T., Rein, D. B., Remuzzi, G., Richardson, K., Rivara, F. P., Roberts, T., Robinson, C., De Leòn, F. R., Ronfani, L., Room, R., Rosenfeld, L. C., Rushton, L., Sacco, R. L., Saha, S., Sampson, U., Sanchez-Riera, L., Sanman, E., Schwebel, D. C., Scott, J. G., Segui-Gomez, M., Shahraz, S., Shepard, D. S., Shin, H., Shivakoti, R., Singh, D., Singh, G. M., Singh, J. A., Singleton, J., Sleet, D. A., Sliwa, K., Smith, E., Smith, J. L., Stapelberg, N. J., Steer, A., Steiner, T., Stolk, W. A., Stovner, L. J., Sudfeld, C., Syed, S., Tamburlini, G., Tavakkoli, M., Taylor, H. R., Taylor, J. A., Taylor, W. J., Thomas, B., Thomson, W. M., Thurston, G. D., Tleyjeh, I. M., Tonelli, M., Towbin, J. A., Truelsen, T., Tsilimbaris, M. K., Ubeda, C., Undurraga, E. A., van der Werf, M. J., van Os, J., Vavilala, M. S., Venketasubramanian, N., Wang, M., Wang, W., Watt, K., Weatherall, D. J., Weinstock, M. A., Weintraub, R., Weisskopf, M. G., Weissman, M. M., White, R. A., Whiteford, H., Wiersma, S. T., Wilkinson, J. D., Williams, H. C., Williams, S. R., Witt, E., Wolfe, F., Woolf, A. D., Wulf, S., Yeh, P. H., Zaidi, A. K., Zheng, Z. J., Zonies, D., Lopez, A. D., Murray, C. J., AlMazroa, M. A., & Memish, Z. A. (2012). Years lived with disability (YLDs) for 1160 sequelae of 289 diseases and injuries 1990-2010: a systematic analysis for the Global Burden of Disease Study 2010. *Lancet*, 380(9859), 2163-2196. http://dx.doi.org/10.1016/S0140-6736(12)61729-2. PMid:23245607.

Yang, S. N. Y., Atkinson, S. C., Wang, C., Lee, A., Bogoyevitch, M. A., Borg, N. A., & Jans, D. A. (2020). The broad spectrum antiviral ivermectin targets the host nuclear transport importin α/β1 heterodimer. *Antiviral Research*, 177, 104760. http://dx.doi.org/10.1016/j.antiviral.2020.104760. PMid:32135219.

Yoshii, S. R., & Mizushima, N. (2015). Autophagy machinery in the context of mammalian mitophagy. *Biochimica et Biophysica Acta*, 1853(10, Pt B), 2797-2801. http://dx.doi.org/10.1016/j.bbamcr.2015.01.013. PMid:25634658.

Youle, R. J., & Narendra, D. P. (2011). Mechanisms of mitophagy. *Nature Reviews. Molecular Cell Biology*, 12(1), 9-14. http://dx.doi.org/10.1038/nrm3028. PMid:21179058.

Zhang, Y. L., Cao, Y. J., Zhang, X., Liu, H. H., Tong, T., Xiao, G. D., Yang, Y. P., & Liu, C. F. (2010). The autophagy-lysosome pathway: a novel mechanism involved in the processing of oxidized LDL in human vascular endothelial cells. *Biochemical and Biophysical Research Communications*, 394(2), 377-382. http://dx.doi.org/10.1016/j.bbrc.2010.03.026. PMid:20223224.